



DISTRIBUTED PHOTOVOLTAIC ELECTRIC SPRING SYSTEM FOR POWER BALANCER IN POWER DISTRIBUTION NETWORKS

PUNATI KIRAN KUMAR¹ N.BALAKRISHNA²

¹PG SCHOLAR, DEPT OF EEE, ESWAR COLLEGE OF ENGINEERING, NARASARAO PET, AP, INDIA

²PROJECT SUPERVISOR, ASSISTANT PROFESSOR, DEPT OF EEE, ESWAR COLLEGE OF
ENGINEERING, NARASARAO PET, AP, INDIA

kirankumarpunati@gmail.com, balakrishnaeee5@gmail.com

Abstract—Electric springs (ES) have been proposed as a demand-response technology for improving the stability and power quality of emerging power systems with high penetration of intermittent renewable energy sources. Existing ES applications mainly involve the regulations of grid voltage and utility frequency. This paper reports a power control and balancing technique for a new integrated configuration of ES and photovoltaic (PV) system, and discusses its possible use to achieve dynamic supply–demand balance in power distribution networks. The proposed system enables delivery of maximally harvested PV power to the grid via the ES, and concurrently controls the active power consumption of its ES associated smart load so as to achieve supply–demand power balance of the overall system in real time. Importantly, battery storage is not necessary in the proposed design because the ES-associated smart-load power follows an appropriate consumption profile to compensate potential prediction errors of the PV power generation. Both simulation and experimental results are included to validate the proposed ES system.

1. INTRODUCTION

Electric power is the most important energy source for human beings. It securely and stably supplies costumers with by power system. A complete power system is consisted of power generators, step-up and step-down transformers, overhead or underground transmission lines and sub transmission lines, distribution cables and switchgear. According to their functions, those components of power system can be categorized into three segments.

The first part is the generation system, in which the electricity is produced from large power plants owned by power companies or independent suppliers. Since the voltage level of the generated power follows the rated voltage setting of generators, in order to transmit the power over long

distance with minimum power loss step-up transformers are utilized to increase the voltage. The second part is the transmission system, the function of transmission system is to deliver the power from generation system to load center via cables or overhead transmission lines. In order to reduce power loss, the power transmitted is at extra high voltage level in both transmission network and subtransmission network. The third part is the distribution system. The power voltage is firstly decreased to medium voltage (MV) level by step-down transformers at terminal substations.

Then the power is transmitted by distribution lines or cables to local substations after its voltage is further reduced to consumer level. At this stage, the electricity can be directly



delivered to residential customers, commercial establishments and industry segments. In order to acquire a better understanding of the physical arrangement of the power system, a typical system which supplies electricity to a big city is taken as an example. In generation stage, the power plants are usually located far away from the urban area to avoid pollution. In transmission stage, the transmission lines or underground cables are used to transmit electricity from the power stations to terminal substations. With increasing awareness on global warming issues and energy crisis, different forms of distributed energy resources (DER) such as photovoltaic (PV) power generations, micro wind turbines, electrical vehicles (EV), and fuel cells have been deployed into power grids over the last decades. With the advantages of a rapidly reduced cost and no rotational parts, PV power generation systems have become an important distributed generation (DG) in low-voltage distribution networks (LV-DNs) for residential and industrial applications. Distributed PV power generation systems are currently growing at an unprecedented speed. In the past decade, the global PV power capacity has surged from 6 GW in 2006 to more than 300 GW in 2016. There are several strategies to address variable generation. The traditional approach is to use dispatchable units already in the system, such as hydropower or conventional fossil-fuelled power plants. An alternative is the use of demand-side management (DSM) techniques, whereby electricity consumption is controlled, either by shedding load or shifting it in time. Storage of electricity, e.g., in batteries

or pumped hydro storage, can also be used to manage variations in generation. Finally, and of most relevance to the present work, variability can be handled using the electric grids.

2. LITERATURE SURVEY

Y. Karimi, H. Oraee, M. S. Golsorkhi, and J. M. Guerrero[1], proposes a new decentralized power management and load sharing method for a photovoltaic based islanded microgrid consisting of various photovoltaic (PV) units, battery units and hybrid PV/battery units. Unlike the previous methods in the literature, there is no need to communication among the units and the proposed method is not limited to the systems with separate PV and battery units or systems with only one hybrid unit. The proposed method takes into account the available PV power and battery conditions of the units to share the load among them. To cover all possible conditions of the microgrid, the operation of each unit is divided into five states and modified active power-frequency droop functions are used according to operating states. The frequency level is used as trigger for switching between the states.

F. Blaabjerg, Y. Yang, D. Yang, and X. Wang[2], Continuously expanding deployments of distributed power-generation systems (DPGSs) are transforming the conventional centralized power grid into a mixed distributed electrical network. The modern power grid requires flexible energy utilization but presents challenges in the case of a high penetration degree of renewable energy, among which wind and solar photovoltaics are typical sources. The integration level of the DPGS into the



grid plays a critical role in developing sustainable and resilient power systems, especially with highly intermittent renewable energy resources. To address the challenging issues and, more importantly, to leverage the energy generation, stringent demands from both utility operators and consumers have been imposed on the DPGS. Furthermore, as the core of energy conversion, numerous power electronic converters employing advanced control techniques have been developed for the DPGS to consolidate the integration. In light of the above, this paper reviews the power-conversion and control technologies used for DPGSs.

X. Wang and Q. Liang[3], As a paradigm of the incoming smart grid, vehicle-to-grid (V2G) has been proposed as a promising solution to increase the adoption rate of plug-in hybrid electric vehicles (PHEVs). In this paper, we investigate the energy management strategies for PHEVs via bidirectional V2G. We first follow a cost-conscious approach from the PHEV owner point of view. To minimize the daily energy cost, we formulate the energy management problem via dynamic programming (DP). However, the “well-known” complexity in solving DP poses a computational challenge even for a small number of iterations. Therefore, we propose a state-independent four-threshold (s, S, s', S') battery charging/discharging policy and theoretically prove the optimality of the proposed energy management strategy based on stochastic inventory theory. A backward iteration algorithm is further developed to practically implement the (s, S, s', S') feedback policy. Second, from the distribution system operator's perspective, we aim to shave the peak

load and flatten the overall load profile. To this end, we propose an optimal PHEV charging scheme and further derive a reminiscent “water-filling” solution for this scenario. Realistic PHEV battery models, time-of-use electricity pricing rate, and real data of household demand are integrated into our formulated V2G system model.

C. Wang, X. Yang, Z. Wu, Y. Che, L. Guo, S. Zhang, and Y. Liu[4], A highly integrated and reconfigurable microgrid testbed is presented in this paper. The microgrid testbed contains various distributed generation units and diverse energy storage systems. Apart from electrical power, it can also provide energy in forms of hydrogen and thermal energy. The topology of this testbed is very flexible with different combinations of buses and feeders. The deployment of hybrid distributed energy sources and the highly reconfigurable structure are available to meet different research requirements. Extensive experiments have been carried out to provide verification for microgrid research and guides for microgrid projects.

Y. Han, H. Li, P. Shen, E. A. A. Coelho, and J. M. Guerrero[5], Microgrids consist of multiple parallel-connected distributed generation (DG) units with coordinated control strategies, which are able to operate in both grid-connected and islanded modes. Microgrids are attracting considerable attention since they can alleviate the stress of main transmission systems, reduce feeder losses, and improve system power quality. When the islanded microgrids are concerned, it is important to maintain system stability and achieve load power sharing among the multiple parallel-connected DG units. However,

the poor active and reactive power sharing problems due to the influence of impedance mismatch of the DG feeders and the different ratings of the DG units are inevitable when the conventional droop control scheme is adopted. Therefore, the adaptive/improved droop control, network-based control methods, and cost-based droop schemes are compared and summarized in this paper for active power sharing. Moreover, nonlinear and unbalanced loads could further affect the reactive power sharing when regulating the active power, and it is difficult to share the reactive power accurately only by using the enhanced virtual impedance method. Therefore, the hierarchical control strategies are utilized as supplements of the conventional droop controls and virtual impedance methods. The improved hierarchical control approaches such as the algorithms based on graph theory, multi-agent system, the gain scheduling method, and predictive control have been proposed to achieve proper reactive power sharing for islanded microgrids and eliminate the effect of the communication delays on hierarchical control.

3 PROBLEM FORMULATION

The high penetration of distributed PV power generation systems in LV-DNs inevitably challenges current ways where the traditional distribution grid is planned and operated. The traditional infrastructure of the power distribution networks is designed to accept only unidirectional power flow from the substation to the households. However, with the distributed PV power generations adopted in LV-DNs, there is a potential reversal of power flow from households to a substation

due to the excessive PV power that may be generated in sunny daytime. Substantial reverse-power flows could cause the problems of over-voltage and grid voltage fluctuations. Such problems may result in incorrect operation of protective devices, damage of grid-tied equipment, reduction in system reliability and utility frequency stability, and even power blackouts. In summary, excessive voltage rise and the supply-demand power imbalance are two emerging problems in increasing deployment of distributed PV systems to the power distribution networks. Various solutions have been suggested to overcome the over-voltage or power imbalance problems. These solutions can be categorized into (i) the traditional tap-changing approaches, (ii) the reactive power compensation, (iii) the PV power generation curtailment, (iv) the adoption of battery energy storage systems (BESS), and (v) the demand-side management.

4.SYSTEM MODELING

A schematic of a PV system connected to the point of common coupling (PCC) is shown in Fig. 4.1. The power grid is represented as a power source V_s including a distribution line Z_{son} on the supply side. A load R_l and a PV system as shown in Fig.4.1 are considered on the demand side. V_g denotes the voltage RMS magnitude of PCC. The PV system is made up of a PV panel array, and an interfacing power inverter that converts and transfers the harvested renewable power (P_{pv}) to the power grid.

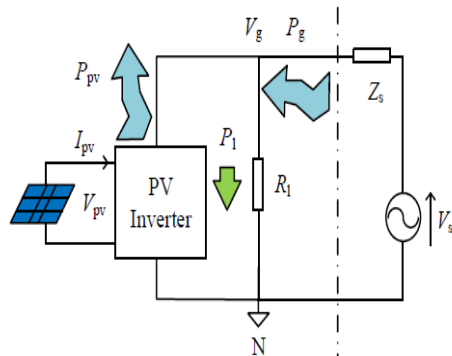


Fig. 1. The simple power grid with a conventional PV system installed. (The zigzag arrows indicate the uncertain power generations while the normal arrow indicates a stable power consumption.)

The load R_1 , consuming a real power P_1 , represents the power consumption on the demand side. The PV power generation at the demand side is predicted as P_{pv_Ref} , and hence an expected supply-side power reference is estimated ($P_{g_Ref} = P_1 - P_{pv_Ref}$). Due to the uncertainty of the PV power generation, the PV power prediction is a great concern for the operators of the energy management in electricity networks with high integration of PV power. Accurate forecasting based on real-time measurements and records is helpful for operators to reduce the impact of the variability of PV power on the grid, and to improve the grid reliability. However, such kinds of forecasting are easily influenced by the external conditions (such as the weather, temperature, and presence of dust). Therefore, the intermittent nature of PV generation still leaves inevitable errors between the predicted power (P_{pv_Ref}) and actual power (P_{pv}). Since the supply-side reference is based on the forecasting, such errors cause the power imbalance between the supply and demand sides.

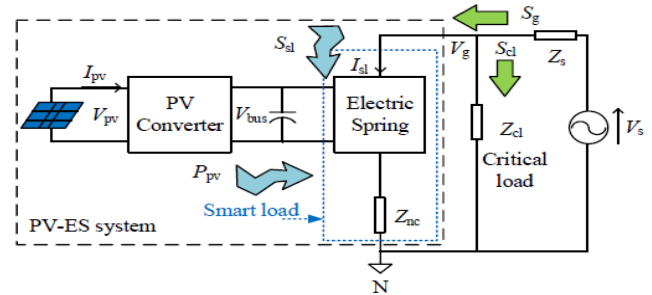


Fig. 2. A simplified diagram of the PV-ES system.

As a supply-demand power balancer, the proposed PV-ES system, as shown in Fig. 4.2, consists of a PV panel array, a PV converter, an ES, and an NC load. In the usual PV harvesting process, the DC power output of the PV converter forms the DC voltage for the ES. The equivalent impedance of the NC load is denoted as Z_{nc} . The remaining loads (not including Z_{nc}) in this power grid can be combined into a single critical load denoted as Z_{cl} . In this paper, we assume a heating or cooling system, which is purely resistive, as the NC load. With the characteristics of (i) being readily available throughout the 24-hour timeframe, (ii) having a great storage inertia in for buffering voltage fluctuation, and (iii) being a widespread appliance commonly available in most of the buildings, such thermal loads are ideal NC candidates for ES applications. The complex power consumed by the ES, the NC load, the critical load, and the ES-associated smart load are respectively denoted as $S_{es} = P_{es} + jQ_{es}$, $S_{nc} = P_{nc} + jQ_{nc}$, $S_{cl} = P_{cl} + jQ_{cl}$, and $S_{sl} = P_{sl} + jQ_{sl}$ (all symbols stand for magnitudes). For the ease of explanation in the subsequent analysis, the critical load is also chosen to be purely resistive ($Q_{nc} = Q_{cl} = 0$). There are two main objectives of using such PV-ES configuration. First,

the ES should regulate the demand-side active power to be a desired value (a value determined by the upper level to maintain a constant power consumption for power balance, or to adjust the power consumption to participate in voltage/frequency regulation, etc.) irrespective of the fluctuation of the PV power generation. Second, the PV system and the ES should collaborate properly in such a way that the system can transfer the intermittent PV power to the grid without the need of battery storage. To handle the desired PV power delivery and to adaptively regulate the power consumption of the smart load simultaneously, two power references, (i) the ES active power reference (P_{es_Ref}) and (ii) the ES-associated smart-load active power reference (P_{sl_Ref}) are required in the proposed control strategy. Based on the assumption that the power loss of the power converters is ignored in the analysis, and the fact that the PV converter is linked to the ES converter as shown in Fig. 4.2, the amount of the harvested PV power (P_{pv}) should be equal to that of the ES active power delivered to the power grid ($-P_{es}$). In the proposed control scheme, the power consumption of the ES-associated smart load should be adjustable irrespective of the PV power fluctuation. The operation point of ES with a given value of P_{sl} can be derived based on the radial-chordal decomposition (RCD) method.

A. Power-Stage Design

The power-stage schematic of the proposed PV-ES system is shown in Fig. 3. The PV interfacing power converter is implemented by an active clamp flyback DC/DC converter, which is used for harvesting PV power with maximum power point tracking

(MPPT) control and stepping up the PV panel voltage (V_{pv}) to be the DC bus voltage (V_{bus}). As shown in Fig. 4.3, the circuit components T1, Sa2, C1, and D1 form a conventional flyback DC/DC power converter. Ca and Sa1 is added to the converter as an active clamp circuit. In addition, D2 and C2 are added to form a voltage multiplier circuit, which doubles the voltage conversion ratio. The input voltage (V_{pv}) and input current (I_{pv}) of this flyback converter are sensed to achieve MPPT.

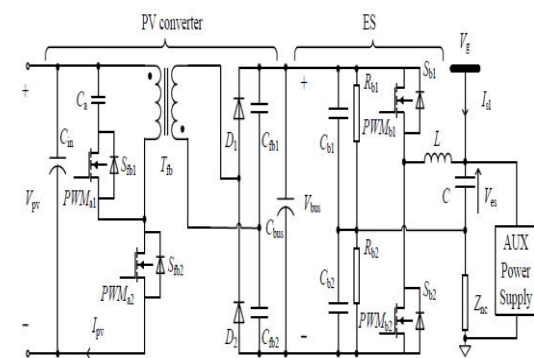


Fig. 3. The power-stage schematic of the proposed PV-ES system.

The ES is realized by a conventional half-bridge DC/AC power converter, which composes C_{b1} , C_{b2} , S_{b1} , and S_{b2} . The DC bus of the ES is connected to the output of the PV interfacing power converter while the AC port of the ES is connected between PCC and the NC load (Z_{nc}). R_{b1} and R_{b2} are added to the power stage of the ES (where $R_{b1} = R_{b2}$) to avoid capacitor voltage imbalance on C_{b1} and C_{b2} . Real-time voltages of V_{bus} , V_{es} , and V_g are sensed and used for the purpose of feedback control. The auxiliary DC power supply for the DSP, sensors, and driver ICs are obtained from the grid AC power, of which the details will not be discussed.

B. Controller Design

The controller design of the PV converter and the ES is discussed in this section. Both the controllers are implemented in a single PWM. The control block diagram of the PV-ES system is shown in Fig. 4.4.

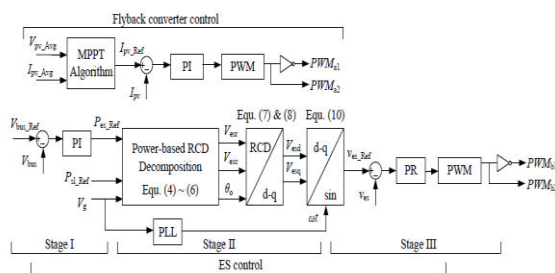


Fig. 4. The control scheme of the PV-ES system.

For the PV converter, the input current (I_{pv}) is regulated by a PI controller. A PV current reference (I_{pv_Ref}) is obtained from the MPPT algorithm. As this paper focuses on the power management rather than the solar power harvesting method, simple PV current-voltage and power-voltage characteristics are considered (in which there is only one maximum power point on the PV power curve), and a current-based incremental conductance algorithm is adopted in this paper for the MPPT control (whose details are omitted). The output signal of the PI controller is used to generate a pair of the 20-kHz complementary PWM signals ($PWMa_1$ and $PWMa_2$) for driving the MOSFET Sa_1 and Sa_2 , respectively. The control process of the ES voltage controller comprises three stages, which are the power reference update (Stage I), the ES voltage reference calculation (Stage II), and the ES voltage regulation (Stage III).

In Stage I, the ES active power reference, P_{es_Ref} , is generated by a PI controller. This PI controller is used to stabilize the DC bus voltage by comparing the sensed V_{bus} with the

constant DC bus reference (V_{bus_Ref}) when the PV converter is operating. Stabilizing V_{bus} requires cooperation of the PV converter and ES. The fluctuation of V_{bus} indicates the power imbalance between the harvested PV power and the real power ES delivered. For example, if V_{bus} is higher than V_{bus_Ref} , it indicates more PV power is harvested than that of ES delivered into the grid, and hence the magnitude of P_{es_Ref} increases in order to restore V_{bus} . Note that when the PV converter is disabled and no PV power is delivered to the output, the ES provides purely reactive power only to control P_{sl} . In this case, the DC voltage is not regulated to V_{bus_Ref} but allowed to vary according to the change of V_{es} . In practice, a θ_0 leading to less reactive power shift may be preferred, as it conducts less transfer of reactive power, and reduces the output voltage of ES. These benefit the DC bus voltage control in Stage I, since the fluctuation caused by reactive power and the voltage-level requirement on components can be reduced. Choosing such a feasible operation point depends on the NC load itself. For instance, if the NC load is capacitive ($\phi_{nc} < 0$), then θ_0 is the sum of the angular components as indicated in (6). In the condition where Z_{nc} is purely resistive, both the choices result in the same level of reactive power shift. Therefore, θ_0 can be alternatively chosen for qualitative compensation using either capacitive- or inductive-reactive power.

5. SIMULATION RESULTS

In this section, the proposed control methodology is first applied to a PV-ES system for a period of 0.4 s that is compressed from a 1 s record. Secondly, the proposed PVES system is compared with the conventional PV

plus BESS(PV+BESS) solution, and that of the three different existing versions of ES.

CASE-A: POWER PROFILES

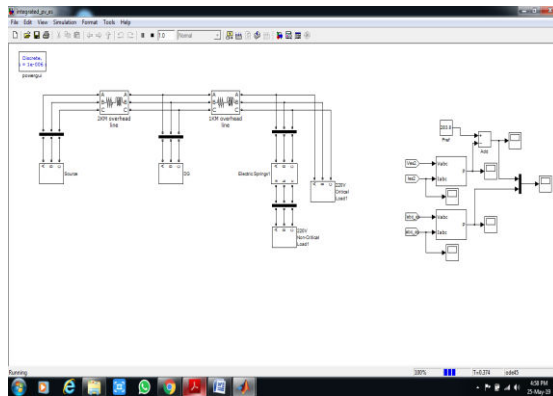


Fig.5. Simulation diagram of ES-PV power profile.

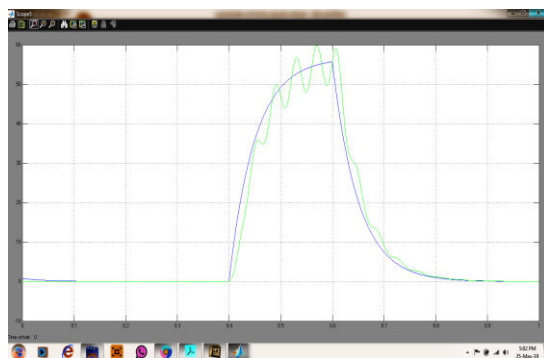


fig.6 The predicted PV power (P_{pv_Ref}) and the actual PV power (P_{pv}).

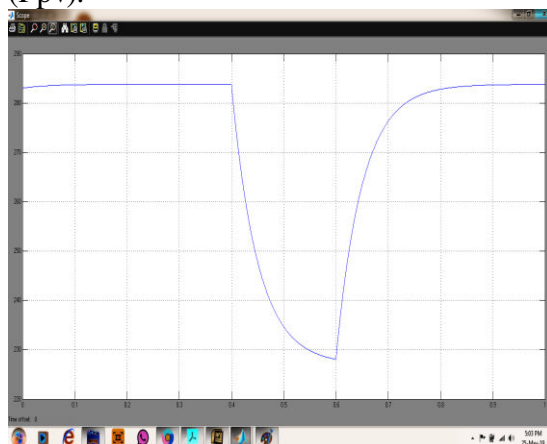


Fig7 The predicted demand-side active power (P_{g_Ref}) reference for the PV-ES system.

The power profiles of the predicted and actual harvested PV power

(P_{pv_Ref} and P_{pv}) used in the simulation are plotted as shown in Fig. 6. The predicted profile of this PV power is forecasted using moving average method based on the data of the solar irradiance. Though the demand-side power reference in practice can be predicted based on various information and objectives, a simple reference for demonstration is calculated by the net amount of the demand-side power. To highlight the power flow control of the PV-ES with fluctuating PV power, Z_{cl} and Z_{nc} are simplified as constant during the simulation period. Hence, the P_{g_Ref} according to shown in Fig.7. Such profiles are then compressed into a period of 1 s for simulation.

CASE-B: PV-ES SYSTEM IN THE FIRST STAGE

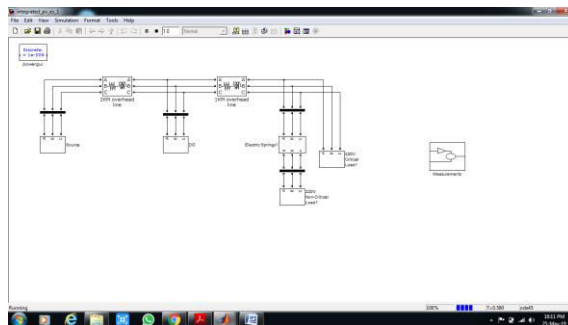
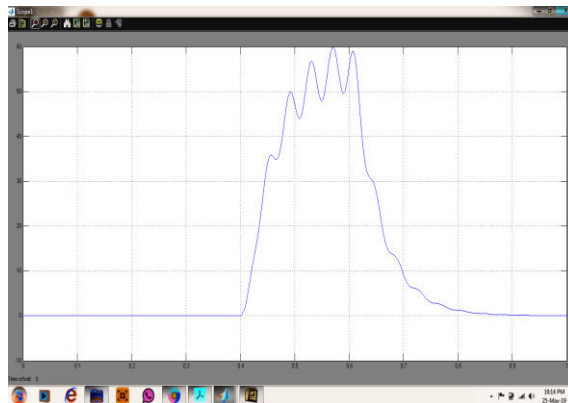
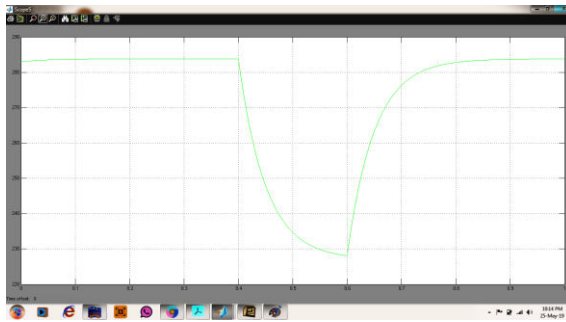


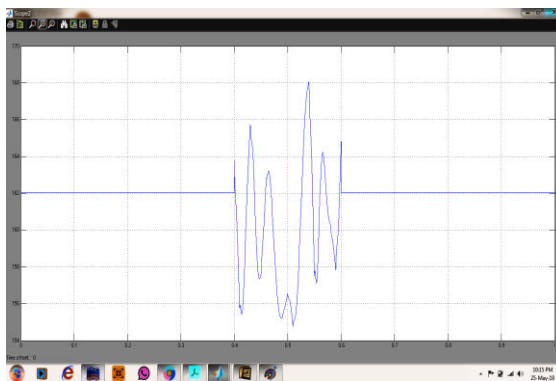
Fig:8. Simulation results of the PV-ES system in the first stage.



fig(a)



fig(b)



fig(c)



fig(d)

Fig.8. Simulation results of the PV-ES system in the first stage. (a) The active power delivered by the ES ($-P_{es}$). (b) The predicted demand-side active power (P_{g_Ref}) and the actual demand-side active power (P_g). (c) The ES reactive power (Q_{es}). (d) The NC load power (P_{nc}).

The simulation results in the first stage are shown in Fig.8. The demand-side power is maintained at the nominal

value between the periods of $t = 0$ s to 0.4 s and $t = 0.6$ s to 1 s, when the PV-ES system is deactivated due to the absence of solar energy. Figure 5.4a shows the time-varying profile of the active power that is delivered to the power grid by the ES ($-P_{es}$). Considering the aforementioned assumption of a lossless converter, the waveform of $-P_{es}$ is exactly of the same shape as that of the actual harvest PV power in Fig. 8a (indicated by the dotted line), which is as expected. In Fig. 8b, the predicted demand-side active power reference (P_{g_Ref}) and the actual simulated demand-side active power (P_g) are plotted together for comparison. The results in Fig. 8b indicate that P_g can be controlled by the PV-ES and it follows precisely the predicted reference. The active power consumption of the NC load in the PV-ES configuration is plotted in Fig. 8c to illustrate that the NC load is indeed operating to compensate the prediction error of the PV power. Clearly, the NC load power is adaptively adjusted closely below and above the nominal power (160 W). In addition, the reactive power transferred by the ES is plotted as shown in Fig. 8d. The negative polarity shows that the ES reactive power is capacitive. By setting the reference of P_{g_Ref} , the reactive power of ES can be made either inductive or capacitive. Here, we arbitrarily choose the capacitive reactive power.

CASE-C: PV+BESS SYSTEM FOR COMPARISON

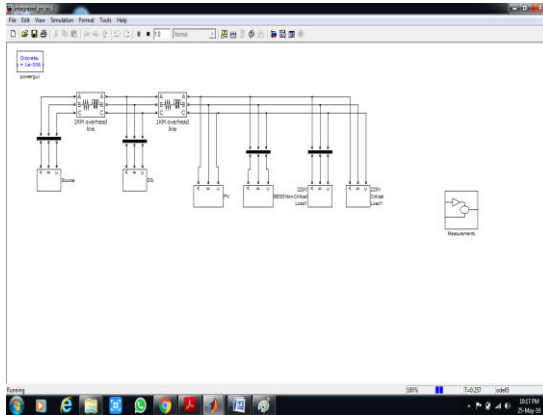
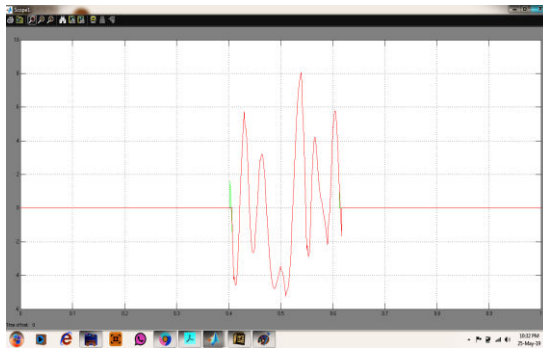
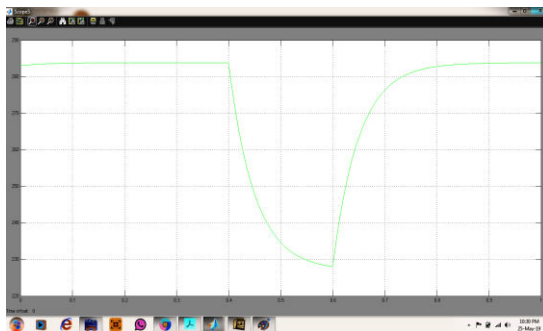


Fig.9. Simulation results of the PV+BESS system for comparison.



fig(a)



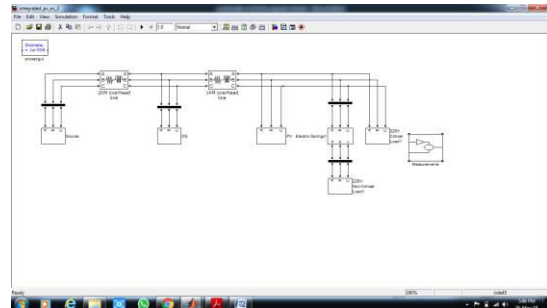
fig(b)

Fig.9. Simulation results of the PV+BESS system for comparison. (a) The active power delivered by the BESS. (b) The actual demand-side active power controlled by the PV+BESS systems.

In the second stage, to compare with the proposed PV-ESS system, the conventional ESS and three existing ES systems solutions for fluctuation

issue of PV power are tested under the same simulation configuration. In the conventional PV+BESS, which is capable of compensating the real power fluctuation by bi-directional power flow, is integrated with the PV inverter either via the DC bus or the PCC. The simulation results of the PV+BESS system are shown in Fig. 9. As shown in Fig. 9a, the ESS directly compensated the error between the predicted and the actual PV power (depicted in Fig. 6a). Hence, the demand-side power is controlled precisely to follow the reference, as shown in Fig. 5.6b. Although the solution of PV+BESS is straightforward and effective in compensating power fluctuation, the installation of BESS is costly. The estimated average cost of BESS installation for commercial scale is \$2,338 USD/kW. For instance, if the maximum prediction error is limited to $\pm 20\%$ of the nominal PV power, a PV system in the scale of 5 kW would require additional \$2,338 USD for the installation of BESS, regardless of future cost on the maintenance of batteries. In contrast, the proposed PV-ES system can save such a cost.

CASE-D: THREE TYPES OF ES SYSTEMS (ES-1, ES-2, AND ES-2B) FOR COMPARISON



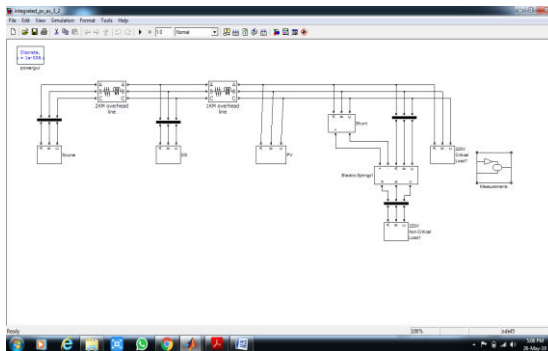
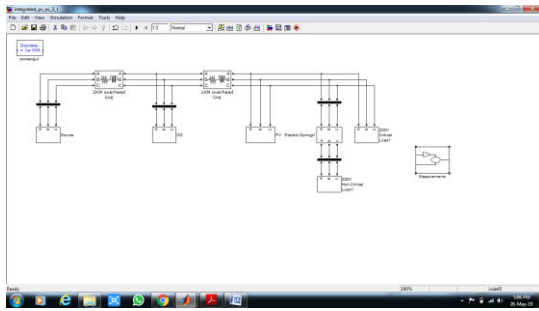
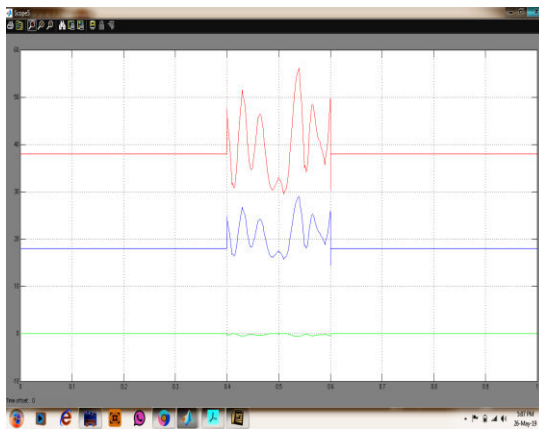


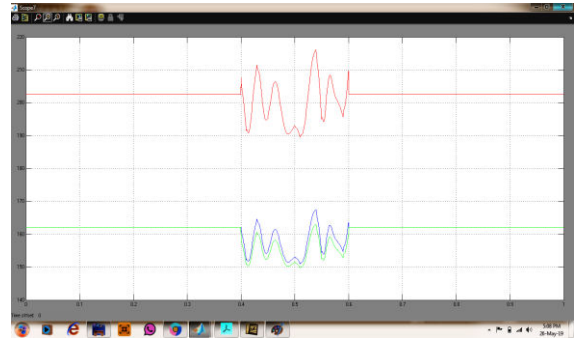
Fig:5.7. Simulation results of the three types of ES systems (ES-1, ES-2, and ES-B2B) for comparison.



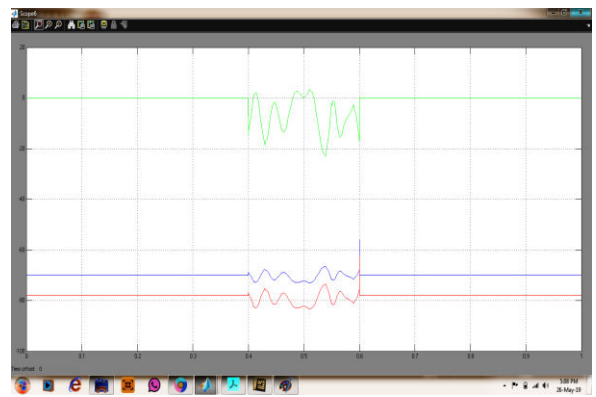
fig(a)



fig(b)



fig(c)



fig(d)

Fig:5.8. Simulation results of the three types of ES systems (ES-1, ES-2, and ES-B2B) for comparison. (a) The active power delivered by the ES systems. (b) The actual demand-side active power controlled by the ES systems. (c) The reactive power consumed by the ES systems. (d) The NC load power in the ES systems.

For comparisons, the objectives of the other three ES systems are set the same as the PV-ES system as a power balancer. Moreover, ES-2 and ES-B2B are preset to regulate the power factor of the smart loads at 0.9. This is a unique function of ES-2 and ES-B2B, which is in contrast to the proposed PV-ES system, since they can be configured to control the active and reactive power consumption simultaneously. Fig. 5.8 shows the simulation results of three ES systems during the period. As observed from Fig. 5.8a, the active power

delivered by ES-1 is almost zero as it can only provide reactive compensation. Fig.5.8b shows the demand-side active power consumption under the regulation of the ES systems. The profiles of ES-2 and ES-B2B illustrates that both these ES are capable of tracking reference as well as the PV-ES. However, the profile of ES-1 contains obvious deviations, which is attributed to the limitation of ES-1. The reason is, with a purely resistive NC load, by providing reactive power, the ES-1 can only decrease (but not increase) the active power consumption of the smart load from the nominal value. Therefore, when the actual PV power is more than the predicted value, the smart load associated with ES-1 cannot consume additional power to compensate the deviation. This is also confirmed by the corresponding NC load consumption and ES reactive power as indicated in Fig. 5.8c and Fig. 5.8d, respectively. As a result, ES-1 cannot achieve the same objective of the proposed PV-ES. Although ES-2 can provide (i) precise active power consumption control of the smart load as well as the PV-ES and (ii) controllable reactive power compensation which is better than the PV-ES, the operation requires real power from its battery storage. As shown in Fig. 5.8a, ES-2 requires around 38W for this 160-W NC load and the maximum-50-W PV generation. Additionally, as shown in Fig. 5.8c, the operation of smart load associated with ES-2 sacrifices the NC load severely. Here, the power of NC load is 198 W at the static state (for power factor regulation) and reaches 224 W during the dynamic state (for both the active power and power factor regulation). In conclusion, while

ES-2 can achieve the same objective as that of the proposed PV-ES, this comes at the expense of a higher cost and poorer performance of the NC load. By contrast, ES-B2B performs the best among the three ES systems in the study. With the same precise active power control of the smart load, the power delivered by the series part of ES-B2B, which is shown in Fig. 5.8a, comes from the grid itself via the shunt ES. According to the power flow of ES-B2B in operation, it possesses a broader range and higher effectiveness in regulating the power consumption than that of ES-2. As depicted in Fig. 5.8a and Fig. 5.8d, the active/reactive power through ES-B2B is smaller than that of ES-2. Also, the power fluctuation of NC load is controlled at the same level as that of PV-ES. In other words, ES-B2B performs as well as the proposed PV-ES as a power balancer.

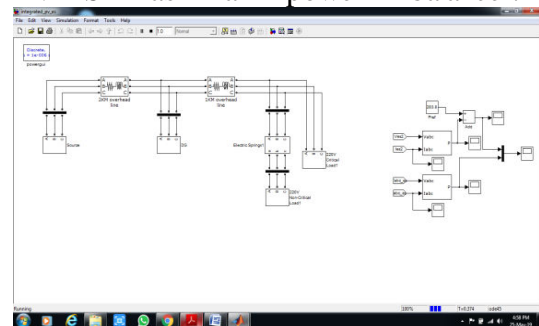


Fig:5.9. Proposed Simulation diagram of ES-PV power profile with fuzzy logic controller

Here we are discussing our proposed improvised control strategy compared with normal electrical spring, i.e. conventional electric spring with improvised electric spring.

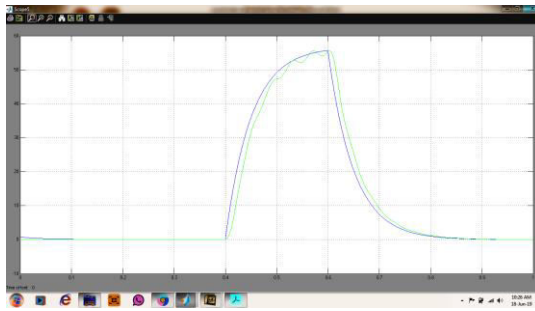


Fig:10. The power profiles of The predicted PV power (P_{pv_Ref}) and the actual PV power (P_{pv}).

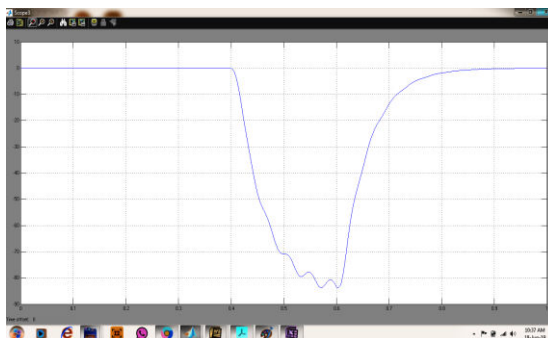
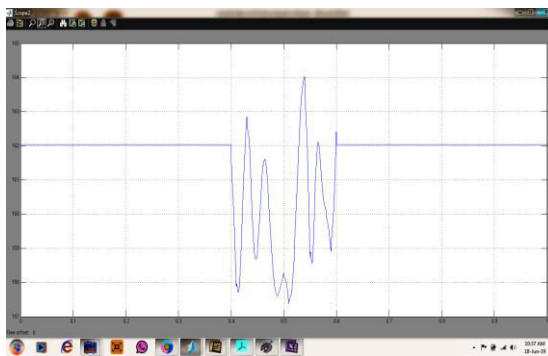
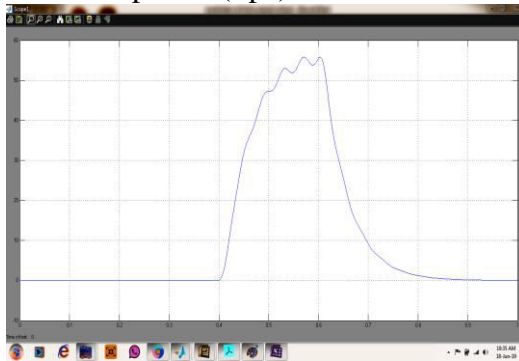


Fig:11 Simulation results of the PV-ES system in the first stage. (a) The active power delivered by the ES ($-P_{es}$). (b) The ES reactive power (Q_{es}). (c) The NC load power (P_{nc}).

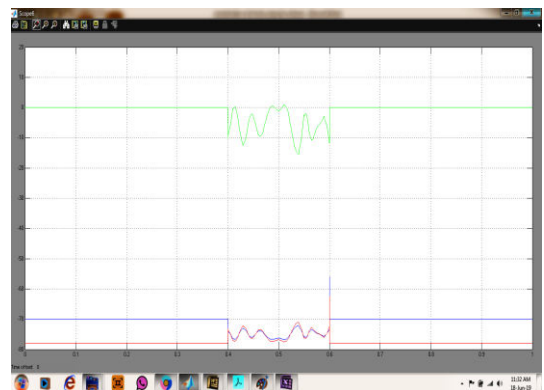
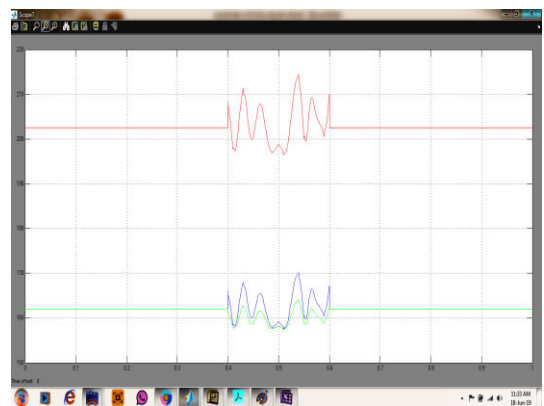
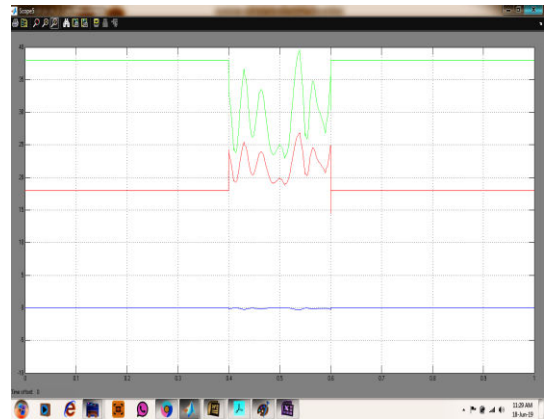


Fig:12 Simulation results of the three types of ES systems (ES-1, ES-2, and ES-B2B) for comparison. (a) The active power delivered by the ES systems. (b) The reactive power consumed by the ES systems. (c) The NC load power in the ES systems.

However, the implementation of fuzzy logic ES-B2B is much higher than that of PVES. While the proposed PV-ES provides a compact configuration including both the PV converter and

the ES inverter, the ES-B2B system requires a back-to-back converter (combined with a shunt and a series ES converters), an isolation transformer, and an individual PV inverter. To summarize, in terms of stabilizing the demand-side power that is influenced by the fluctuating PV power, the proposed PV-ES system performs as well as, if not better than, the other options currently available. However, the low implementation cost of its converter circuit and its battery-free configuration makes it much more competitive as a practical solution. If deployed in a power system with existing ESS, diesel generators and load control strategies, the PV-ES will further benefit the system: (i) PV-ES will be compatible with common load control strategies as it provides continuous power flow adjustment as a smart load; (ii) PV-ES may help to reduce the requirement of the rating power of ESS and diesel generators, as it mitigates the power fluctuation of PV power.

CONCLUSION

In this project, a PV-ES system that is acting as a power balancer, is adopted in power distribution networks that have a high penetration of PV power generations, to assist in grid stabilization. The power flow analysis and implementation design in single-phase power system ensure that the proposed PV-ES can harvest the fluctuating MPPT PV power without involving battery storage, and adaptively control the active power consumption of the ES-associated smart load simultaneously. A comparison of the proposed PV-ES solution with the conventional BESS solution and those based on previous types of ES, validates that the former is a relatively better solution with a lower

installation cost. Among proposed ES circuits, the ES-B2B should be the most prominent candidate in fulfilling this task, since the shunt and series inverters are both able to generate reactive power. The research can commence from the study of control technique with the use of a single ES-B2B and then escalate to the investigation of the joint performance of large-scale distributed ES-B2Bs. The application of fuzzy logic controller on the regulation of distributed ESs is a central approach which requires one-way communication for the broadcast of the control command to individual components. However, the difficulty lies on the derivation of a robust system model that can tolerate the plug-and-play feature of ES.

REFERENCES

- [1] T. Kerekes, R. Teodorescu, M. Liserre, C. Klumpner, and M. Sumner, "Evaluation of three-phase transformerless photovoltaic inverter topologies," *IEEE Transactions on Power Electronics*, vol. 24, no. 9, pp. 2202–2211, Sep. 2009.
- [2] Y. Karimi, H. Oraee, M. S. Golsorkhi, and J. M. Guerrero, "Decentralized method for load sharing and power management in a PV/battery hybrid source islanded microgrid," *IEEE Transactions on Power Electronics*, vol. 32, no. 5, pp. 3525–3535, 2017.
- [3] F. Blaabjerg, Z. Chen, and S. B. Kjaer, "Power electronics as efficient interface in dispersed power generation systems," *IEEE Transactions on Power Electronics*, vol. 19, no. 5, pp. 1184–1194, Sep. 2004.
- [4] F. Blaabjerg, Y. Yang, D. Yang, and X. Wang, "Distributed power generation systems and protection," *Proceedings of the IEEE*,



- vol. 105, no.7, pp. 1311–1331, Jul. 2017.
- [5] W. Kempton and J. Tomic, “Vehicle-to-grid power implementation: From stabilizing the grid to supporting large-scale renewable energy,” *J. Power Sources*, vol. 144, no. 1, pp. 280–294, Jun. 2005.
- [6] X. Wang and Q. Liang, “Energy management strategy for plug-in hybrid electric vehicles via bidirectional vehicle-to-grid,” *IEEE Systems Journal*, vol. 11, no. 3, pp. 1789–1798, Sep. 2017.
- [7] C. Wang, X. Yang, Z. Wu, Y. Che, L. Guo, S. Zhang, and Y. Liu, “A highly integrated and reconfigurable microgrid testbed with hybrid distributed energy sources,” *IEEE Transactions on Smart Grid*, vol. 7, no.1, pp. 451–459, Jan. 2016.
- [8] Y. Han, H. Li, P. Shen, E. A. A. Coelho, and J. M. Guerrero, “Review of active and reactive power sharing strategies in hierarchical controlled microgrids,” *IEEE Transactions on Power Electronics*, vol. 32, no. 3, pp. 2427–2451, 2017.
- [9] S. B. Kjaer, J. K. Pedersen, and F. Blaabjerg, “A review of single-phase grid-connected inverters for photovoltaic modules,” *IEEE Transactions on Industry Applications*, vol. 41, no. 5, pp. 1292–1306, Sep. 2005.
- [10] F. Olivier, P. Aristidou, D. Ernst, and T. Van Cutsem, “Active management of low-voltage networks for mitigating overvoltages due to photovoltaic units,” *IEEE Transactions on Smart Grid*, vol. 7, no. 2, pp. 926–936, 2016.
- [11] C. Whitaker, J. Newmiller, M. Ropp, and B. Norris, “Renewable systems interconnection study: distributed photovoltaic systems design and technology requirements,” Sandia National Laboratories, Albuquerque, New Mexico 87185 and Livermore, California, Tech. Rep. SAND2008-0946 P, 2008.
- [12] Y. Yang, H. Li, A. Aichhorn, J. Zheng, and M. Greenleaf, “Sizing strategy of distributed battery storage system with high penetration of photovoltaic for voltage regulation and peak load shaving,” *IEEE Transactions on Smart Grid*, vol. 5, no. 2, pp. 982–991, 2014.
- [13] REN21 Secretariat, *Renewables 2017: Global Status Report*. (2017). REN21. [Online]. Available: http://www.ren21.net/wpcontent/uploads/2017/06/17-8399_GSR_2017_Full_Report_0621_Opt.pdf.
- [14] R. Margolis, D. Feldman, and D. Boff. (2017, Apr.). Q4 2016/Q1 2017 Solar Industry Update. Sunshot, U.S. Department of Energy. [Online]. Available: <https://www.nrel.gov/docs/fy17osti/68425.pdf>.
- [15] *Renewables 2017: Analysis and Forecasts to 2022 Executive Summary*. (2017, Oct.) International Energy Agency. [Online]. Available: <https://www.iea.org/Textbasenpsum/renew2017MRSsum.pdf>.
- [16] J. D. Glover, M. S. Sarma, and T. Overbye, *Power System Analysis and Design*, Fifth Edition, 5th ed. Stamford, CT: Cengage Learning, Jan. 2011.
- [17] C. L. Masters, “Voltage rise: the big issue when connecting embedded generation to long 11 kV overhead lines,” *Power Engineering Journal*, vol. 16, no. 1, pp. 5–12, Feb. 2002.
- [18] R. A. Walling, R. Saint, R. C. Dugan, J. Burke, and L. A. Kojovic, “Summary of distributed



resources impact on power delivery systems," IEEE Transactions on Power Delivery, vol. 23, no. 3, pp. 1636–1644, Jul. 2008.

[19] Q. Fu, L. F. Montoya, A. Solanki, A. Nasiri, V. Bhavaraju, T. Abdallah, and D. C. Yu, "Microgrid generation capacity design with renewables and energy storage addressing power quality and surety," IEEE Transactions on Smart Grid, vol. 3, no. 4, pp. 2019–2027, Dec. 2012.

[20] X. Liu, A. Aichhorn, L. Liu, and H. Li, "Coordinated control of distributed energy storage system with tap changer transformers for voltage rise mitigation under high photovoltaic penetration," IEEE Transactions on Smart Grid, vol. 3, no. 2, pp. 897–906, Jun. 2012.

[21] T. T. Hashim, A. Mohamed, and H. Shareef, "A review on voltage control methods for active distribution networks," Prz. Elektrotech, vol. 88, pp. 304–312, 2012.

[22] T. Stetz, F. Marten, and M. Braun, "Improved low voltage grid-

integration of photovoltaic systems in Germany," IEEE Transactions on Sustainable Energy, vol. 4, no. 2, pp. 534–542, Apr. 2013.

[23] R. Tonkoski, L. A. C. Lopes, and T. H. M. El-Fouly, "Coordinated active power curtailment of grid connected PV inverters for overvoltage prevention," IEEE Transactions on Sustainable Energy, vol. 2, no. 2, pp. 139–147, Apr. 2011.

[24] S. Alyami, Y. Wang, C. Wang, J. Zhao, and B. Zhao, "Adaptive real power capping method for fair overvoltage regulation of distribution networks with high penetration of pv systems," IEEE Transactions on Smart Grid, vol. 5, no. 6, pp. 2729–2738, 2014.

[25] M. Zillmann, R. Yan, and T. K. Saha, "Regulation of distribution network voltage using dispersed battery storage systems: a case study of a rural network," in Proc. 2011 IEEE Power and Energy Society General Meeting, Jul. 2011, pp. 1–8.